Synthetic and Systems Biotechnology 8 (2023) 107–113

Contents lists available at ScienceDirect

Synthetic and Systems Biotechnology

journal homepage: www.keaipublishing.com/en/journals/synthetic-and-systems-biotechnology

Original Research Article

Engineered geranyl diphosphate methyltransferase produces 2-methyl-dimethylallyl diphosphate as a noncanonical C_6 unit for terpenoid biosynthesis

Chen-Yang Xia [a], Bo-Wen Lu [a], Ji-Yun Cui [a], Bai-Yang Wang [a], Yue-Yang Sun [a], Fei Gan [a,b,c,*]

[a] Hubei Key Laboratory of Cell Homeostasis, College of Life Science, Wuhan University, Wuhan, China
[b] TaiKang Center for Life and Medical Science, Wuhan University, Wuhan, China
[c] Hubei Provincial Cooperative Innovation Center of Industrial Fermentation, Wuhan, China

ARTICLE INFO

Keywords:
Protein engineering
Terpenoid biosynthesis
Methyltransferase
Noncanonical building block

ABSTRACT

Terpenoids constitute the largest class of natural products with complex structures, essential functions, and versatile applications. Creation of new building blocks beyond the conventional five-carbon (C_5) units, dimethylallyl diphosphate (DMAPP) and isopentenyl diphosphate, expands significantly the chemical space of terpenoids. Structure-guided engineering of an *S*-adenosylmethionine-dependent geranyl diphosphate (GPP) C2-methyltransferase from *Streptomyces coelicolor* yielded variants converting DMAPP to a new C_6 unit, 2-methyl-DMAPP. Mutation of the Gly residue at the position 202 resulted in a smaller substrate-binding pocket to fit DMAPP instead of its native substrate GPP. Replacement of Phe residue at the position 222 with a Tyr residue contributed to DMAPP binding via hydrogen bond. Furthermore, using *Escherichia coli* as the chassis, we demonstrated that 2-methyl-DMAPP was accepted as a start unit to generate noncanonical *trans*- and *cis*-prenyl diphosphates (C_{5n+1}) and terpenoids. This work provides insights into substrate recognition of prenyl diphosphate methyltransferases, and strategies to diversify terpenoids by expanding the building block portfolio.

1. Introduction

Terpenoids constitute a large group of natural products with complex structures, and are important sources of biofuels, flavors, cosmetics, fragrances, and especially pharmaceuticals (e.g., artemisinin, paclitaxel, canabinoids) [1–4]. Despite the structural diversity, terpene biosynthesis builds up on two fundamental five-carbon (C_5) molecules: dimethylallyl diphosphate (DMAPP) and isopentenyl diphosphate (IPP). Condensation of DMAPP and IPP leads to prenyl diphosphates of different length including geranyl diphosphate (GPP, C_{10}), farnesyl diphosphate (FPP, C_{15}), geranylgeranyl diphosphate (GGPP, C_{20}), geranylfarnesyl diphosphate (GFPP, C_{25}), hexaprenyl diphosphate (HexPP, C_{30}), and longer C_{5n} molecules, which are processed by terpene synthases into acyclic or cyclic terpenes [5–8]. Of note, using an efficient yeast-based genome mining platform, two fungal chimeric triterpene synthases were recently discovered to convert DMAPP and IPP through HexPP into triterpenes, presenting a non-squalene-dependent route for triterpene biosynthesis [7]. The terpene scaffolds can be further decorated by enzymes including cytochrome P450s and transferases. The so-called isoprene rule applies strictly to terpene biosynthesis, and only a few exceptions have been reported. Examples include incorporation of C_6 homo-IPP and homo-DMAPP into juvenile hormones in lepidoptera [9], methylation of FPP at C10 and cyclization to produce pre-sodorifen diphosphate during sodorifen biosynthesis [10], and synthesis of 2-methyl-GPP, 6-methyl-GPP, and (*Z*)-homo-IPP by *S*-adenosylmethionine (SAM)-dependent methyltransferases as the precursor of 2-methylisoborneol [11–13], benzastatin [14], and longestin [15], respectively. These uncommon prenyl diphosphate precursors lead to biosynthesis of terpenoids with novel structures in microbial hosts including *Escherichia coli* and *Saccharomyces cerevisiae* [9,16–19].

Presumably, modification at the earliest step of terpenoid synthesis (i.e., C_5 diphosphates) contributes most significantly to extend the chemical space. Systematic genome mining of a prenyl diphosphate methyltransferase recently revealed homologs that transform IPP into several C_6 and C_7 compounds [20,21]. Nevertheless, the enzyme that converts DMAPP into 2-methyl-DMAPP has not yet been discovered, nor

Peer review under responsibility of KeAi Communications Co., Ltd.
* Corresponding author. Bayi Rd. 299, Wuchang, Wuhan, Hubei, 430072, China
E-mail address: feigan@whu.edu.cn (F. Gan).

https://doi.org/10.1016/j.synbio.2022.12.002
Received 1 October 2022; Received in revised form 11 December 2022; Accepted 12 December 2022
Available online 19 December 2022

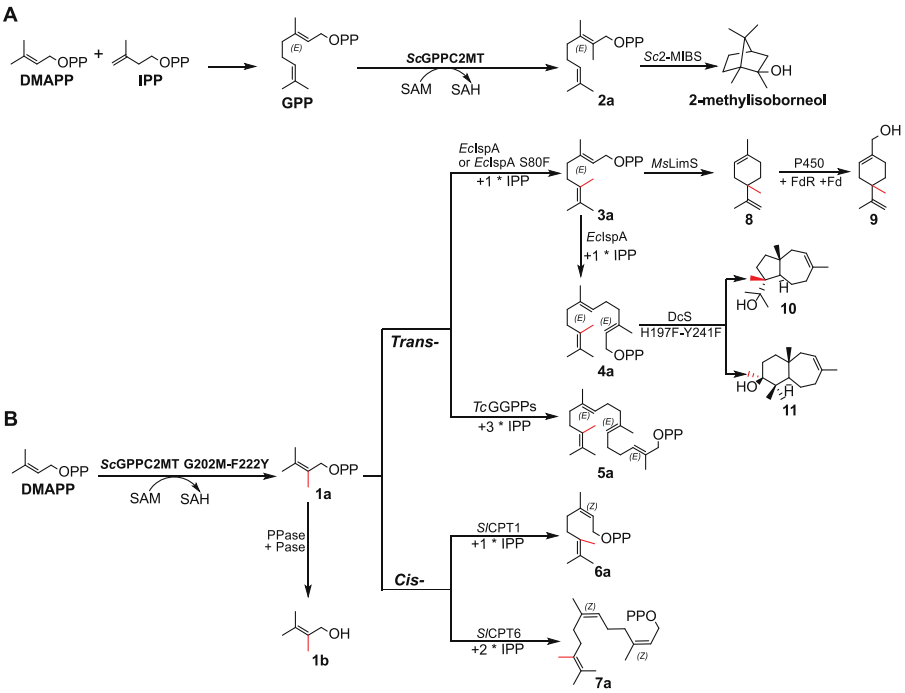

Fig. 1. Synthesis of 2-methyl-DMAPP as a noncanonical C_6 building block for terpenoid biosynthesis. (**A**) The SAM-dependent methyltransferase *Sc*GPPC2MT converts GPP to 2-methyl-GPP (**2a**), the precursor of 2-methylisoborneol. *Sc*: *Streptomyces coelicolor*. (**B**) Engineered *Sc*GPPC2MT variant G202M-F222Y transforms DMAPP to 2-methyl-DMAPP (**1a**), a precursor for 6-methyl-GPP (**3a**), 10-methyl-*E, E*-FPP (**4a**), 14-methyl-*E, E, E*-GGPP (**5a**), 6-methyl-NPP (**6a**), 10-methyl-*Z, Z*-FPP (**7a**), C_{11} (**8**, **9**) and C_{16} terpenoids (**10**, **11**). Due to endogenous phosphatase activities, prenyl diphosphates can be converted to alcohols (e.g., 2-methyl-prenol, **1b**).

terpenoid biosynthesis involving 2-methyl-DMAPP has been reported.

In this study, we aim to engineer prenyl diphosphate methyltransferases to produce noncanonical substrate, 2-methyl-DMAPP in this study, for terpenoid biosynthesis (Fig. 1). The SAM-dependent methyltransferase that converts GPP to 2-methyl-GPP [11–13], GPPC2MT, was chosen as the model enzyme. Pathways built upon the newly created DMAPP C2-methyltransferase and downstream enzymes including terpene synthases and cytochrome P450s were integrated into *Escherichia coli*, to explore application of 2-methyl-DMAPP as a start unit for terpenoid biosynthesis.

2. Material and methods

2.1. Strains, plasmids, and reagents

Escherichia coli strain DH5α (Takara) was used for recombinant plasmid construction. To obtain high levels of DMAPP and IPP in *E. coli* cells, the plasmid pTS1 was made to express the whole mevalonate pathway including acetoacetyl-CoA synthase, hydroxymethylglutaryl (HMG)-CoA synthase, HMG-CoA reductase, mevalonate kinase, phosphomevalonate kinase, phosphomevalonate decarboxylase and isopentenyl diphosphate isomerase. Two vectors with compatible replication origins, pTS2 and pTS3, were constructed to afford gene expression. Gene of interest (e.g., encoding the GPP C2-methyltransferase, terpene synthase) was inserted into pTS2 or pTS3, and the resulting recombinant plasmids (Table S1 and Fig. S1) were transformed into *E. coli* BL21 (DE3) (Novagen) separately or in combination for protein expression and terpenoid production. All primers used for recombinant plasmid construction were listed in Table S2. Sources and sequences of enzymes involved were summarized in Tables S3 and S4. Detailed description of plasmid construction and reagents were included in supporting information.

2.2. Sequence alignment and homology modeling

The GPPC2MTs from *Streptomyces coelicolor* (*Sc*GPPC2MT, PDB: 3VC2) and *Streptomyces lasaliensis* (PDB: 4F84) and isopentenyl diphosphate methyltransferases from *Streptomyces monomycini* (*Sm*IPPMT, WP_033037353.1), *Rhodococcus fascians* (WP_015586130.1 & WP_032387891.1), and *Nocardia brasiliensis* (WP_014984011.1) were aligned with ClustalW integrated in MEGA XI [22]. Structural modeling of the *Sc*GPPC2MT variant was performed with SWISS-MODEL [23] using the wild type as a template. Docking of DMAPP into substrate-binding pocket of *Sc*GPPC2MT variant was performed with AutoDockTools [24]. All structures were illustrated using PyMOL 2.5 [25] and ProterinsPlus (https://Proteins.Plus) [26].

2.3. Production of prenyl diphosphates and terpenoids

Recombinant plasmids were transformed into *E. coli* BL21(DE3) for prenyl diphosphate and terpenoid production (Table S5). A single colony was inoculated in LB medium (1% (w/v) tryptone, 0.5% (w/v) yeast extract, 1% (w/v) NaCl) with appropriate antibiotics (e.g., 100 μg/mL ampicilin, 30 μg/mL chloramphenicol, 12.5 μg/mL kanamycin) and cultivated overnight at 37°C with shaking at 200 rpm. The start culture was diluted into 50 mL TB medium (1.2% (w/v) tryptone, 2.4% (w/v) yeast extract, 0.4% (v/v) glycerol) supplemented with appropriate antibiotics, 3 g/L L-methionine and additional 0.4% (v/v) glycerol to an OD_{600} = 0.1. When OD_{600} = 1.0, protein expression was induced by adding 0.1 mM isopropyl β-D-1-thiogalactopyranoside (IPTG) and, when needed, 10 mM L-arabinose. The venthole of the culture-containing flasks was sealed. Cultures were maintained at 30°C for 24 h (for analysis of C_6, C_{11}, and C_{16} prenyl diphosphates) or at 18°C for 72–96 h (for analysis of C_{21} prenyl diphosphate, terpenoids, and yield of 2-methyl-prenol in the presence of NudB) before harvesting. Products were extracted by adding 4 mL of *n*-hexane into 43.5 mL of cultures and vortexing rigorously. After centrifugation, 3 mL of organic phase was collected, supplemented with 10-undecen-1-ol as the internal standard, and concentrated to 300 μL for gas chromatography-mass spectrometry (GC-MS) analysis.

2.4. Enzyme expression and purification

To purify wild type *Sc*GPPC2MT and its variant G202M-F222Y for *in vitro* activity assay, a single colony of *E. coli* BL21 (DE3) carrying pTS10 or pTS10V was inoculated in LB containing kanamycin (50 μg/mL) and

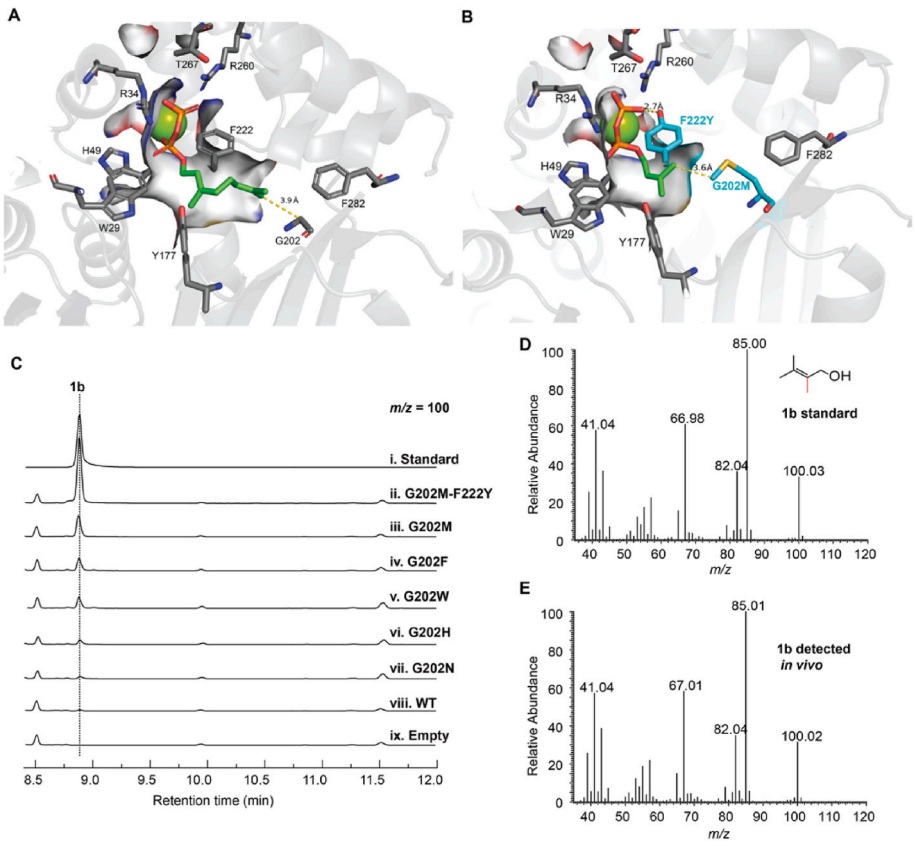

Fig. 2. Engineering *Sc*GPPC2MT to make 2-methyl-DMAPP. (**A**) Structure of *Sc*GPPC2MT in complex with its native substrate GPP (PDB:3VC2). (**B**) Model structure of *Sc*GPPC2MT variant G202M-F222Y in complex with DMAPP. The G202M and F222Y are colored in cyan. (**C**) Analysis of 2-methyl-prenol (**1b**) produced by *Sc*GPPC2MT variants. (**D** and **E**) Mass spectrum of **1b** standard (**D**) and produced *in vivo* (**E**).

grown at 37°C. The start culture was subcultured into fresh medium and protein expression was induced by 0.1 mM IPTG and carried at 18°C. Harvested cells were washed and resuspended with buffer A (50 mM Tris, 300 mM NaCl, 10% (v/v) glycerol, pH 7.5), disrupted by sonication, and centrifuged at 4°C. The resulting supernatant was filtered through a 0.22 μm membrane and loaded on to a column of Ni-NTA resin (Qiagen). After washing with buffer A supplemented with 80 mM imidazole, the target protein was eluted with buffer A containing 250 mM imidazole, and dialyzed into buffer B (50 mM PIPES, 100 mM NaCl, 15 mM $MgCl_2$, 10% (v/v) glycerol, pH 6.7) for storage. Purity and concentration of obtained protein samples was analyzed by SDS-PAGE and Bradford assay.

2.5. In vitro activity assay

For *in vitro* activity assay, each reaction containing 20 μM *Sc*GPPC2MT wild type or variant, 60 μM DMAPP or GPP, and 60 μM SAM in reaction buffer (50 mM Tris-HCl, 100 mM NaCl, 20% (v/v) glycerol, 10 mM $MgCl_2$, 2 mM EDTA, 0.2 mM DTT, pH 8.0) was incubated at 30°C for 24 h, terminated by adding 0.5 M EDTA (pH 8.0), and further treated with acid phosphatase (pH 4.8) at 37°C for 24 h. The volatile products in the headspace were extracted with a d_f 85 μm solid phase microextraction fiber, followed by GC-MS. Hydrolyzed products were extracted with *n*-hexane and also analyzed by GC-MS [27].

Steady-state kinetics were assayed by measuring formation of *S*-adenosylhomocysteine (SAH). Each reaction consisting of wild type *Sc*GPPC2MT (2 μM) with variable GPP (0–30 μM) or variant G202M-F222Y (5 μM) with variable DMAPP (0–60 μM) in 100 μL reaction buffer (50 mM PIPES, 20% (v/v) glycerol, 10 mM $MgCl_2$, 100 mM NaCl, 5 mM 2-mercaptoethanol, 100 μM SAM, pH 7.0) was kept at 30°C for 20 min, and quenched by methanol. The supernatant fractions after centrifugation were analyzed by high-performance liquid chromatography system (Chromaster, HITACHI) connected with a C18 column (L:4.6 mm × D:250 mm, LaChrom) using a linear gradient (5%–100%) of acetonitrile containing 20 mM ammonia acetate and a flowrate of 0.8 mL/min. The formed SAH was quantified according to a standard curve of SAH standard drawn by measuring the absorbance at 254 nm [14,28].

2.6. GC-MS analysis

GC-MS analysis was performed on a Trace^{TM} 1300-TSQ 8000 Evo system (Thermo Fisher Scientific) connected with a TG-5MS column (L:30 m × D:0.25 mm, Thermo Fisher Scientific) at a helium flow of 1 mL/min. The inlet temperature and the MS transfer line temperature was 250°C. 1 μL of sample was injected using splitless mode, and split 1:20 after 1 min. For analysis of C_6, C_{11}, and C_{16} prenyl alcohols, the program was set as 40°C for 6.5 min, 30°C/min to 55°C and hold for 5 min, 50°C/min to 125°C, 3°C/min to 145°C, 50°C/min to 170°C, 3°C/min to 190°C, 50°C/min to 210°C, 3°C/min to 230°C, 50°C/min to 250°C, and hold for 7 min. For analysis of C_{21} prenyl alcohols and terpenoids, the program was set as 40°C for 6.5 min, 50°C/min to 85°C, 3°C/min to 105°C, 50°C/min to 160°C, 3°C/min to 230°C, 50°C/min to 250°C, and hold for 7 min. GC-MS data were collected and processed with Xcalibur (Thermo Fisher Scientific). Compounds were identified with standard molecules synthesized or reported in references, and NIST mass spectral library.

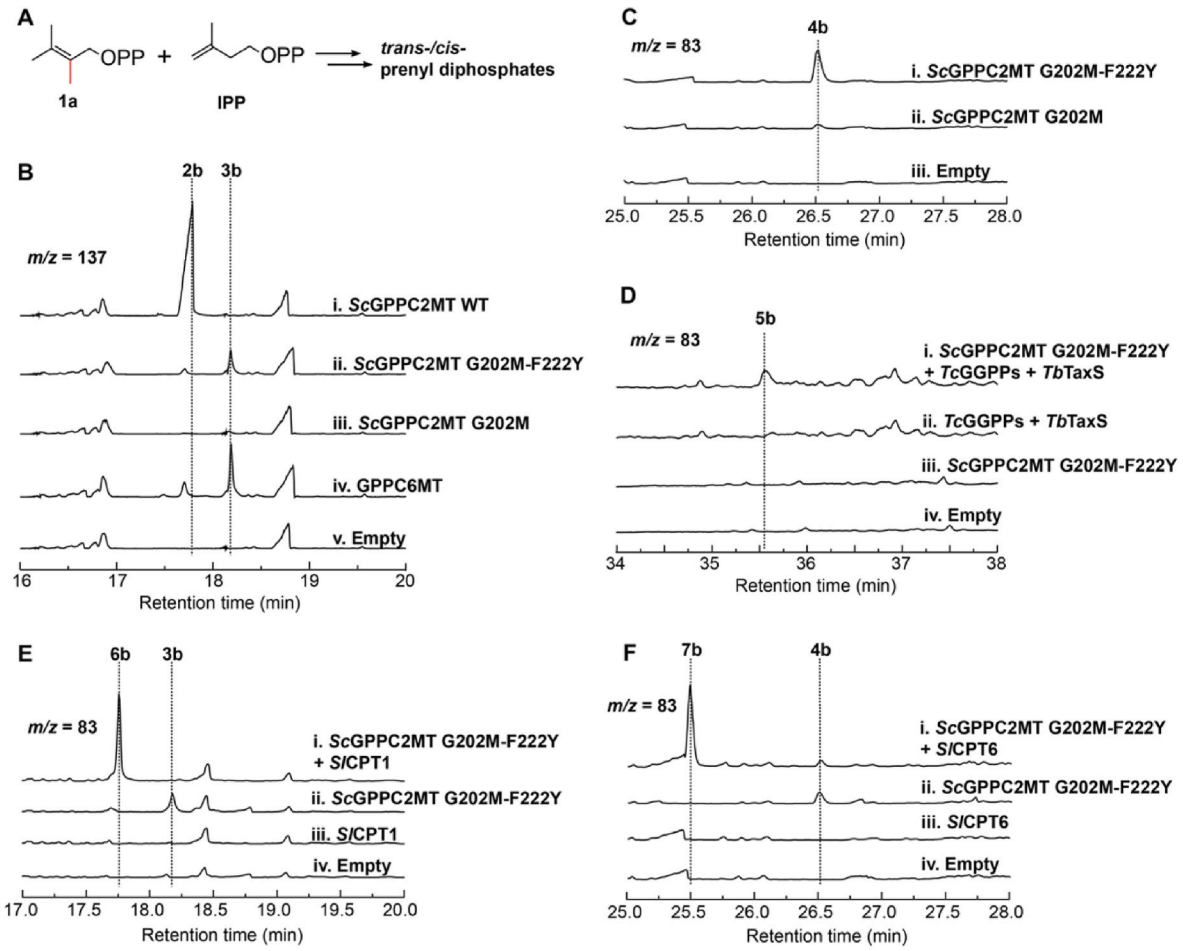

Fig. 3. Incorporation of 2-methyl DMAPP into prenyl diphosphates. (**A**) Condensation of 2-methyl-DMAPP (**1a**) with IPP to generate *trans*- or *cis*-prenyl diphosphates. (**B**) Analysis of 2-methyl-geraniol (**2b**) and 6-methyl-geraniol (**3b**). (**C**) Analysis of 10-methyl-*E, E*-farnesol (**4b**) production. (**D**) Production of 14-methyl-*E, E, E*-geranylgeraniol (**5b**) by co-expressing variant G202M-F222Y, *Tc*GGPPs, and *Tb*TaxS. (**E** and **F**) Analysis of 6-methyl-nerol (**6b**) and 10-methyl-*Z, Z*-farnesol (**7b**) upon co-expression of the variant G202M-F222Y with *Sl*CPT1 (**E**) and with *Sl*CPT6 (**F**) respectively. The target molecule was not detected in control group harboring empty vector(s) (empty) or expressing incomplete combination of enzymes.

3. Results and discussion

3.1. Engineering GPP C2-methyltransferase to use DMAPP as a new substrate

In term of molecular structures, the C2 of GPP is analogous to C2 of DMAPP; however, no methylated DMAPP is produced by GPPC2MT. Indeed, GPPC2MT exhibits strict substrate specificity towards GPP. Crystal structure of *Sc*GPPC2MT in complex with GPP shows that the diphosphate group coordinates to Mg^{2+} ion and interacts with R34, H49, Y51, and R260 via hydrogen bond, while the hydrocarbon tail extends into a groove defined by W29, H49, Y51, E173, M176, Y177, I218, F222, C224, I226, F273, Y277, F282, and Y284 [27]. We reasoned that the GPP-binding groove is large for DMAPP, and engineering the groove to fit DMAPP is necessary. Examination of amino acid residues at the binding pocket led to G202, located at the bottom of GPP-binding groove and is 3.9 Å away from the prenyl chain (Fig. 2A). Interestingly, in SAM-dependent IPP methyltransferases, a conserved Trp residue, W194, occupies the parallel position (Fig. S2), and is considered to fix the hydrocarbon chain of IPP in the active site pocket [20]. We reasoned that substitution of G202, the smallest amino acid residue, with ones of appropriate side groups would narrow the binding groove to accommodate DMAPP. Therefore, G202 was subject to site-saturation mutagenesis. The resulting *Sc*GPPC2MT variants G202X (X denotes residue other than G) were assayed for 2-methyl-DMAPP synthesis in *E. coli*. Because endogenous phosphatases (e.g., NudB) exhibit substrate promiscuity towards prenyl diphosphates [29–31], prenyl alcohols in production runs was analyzed by gas chromatography-mass spectrometry (GC-MS).

To setup the *in vivo* production assay, we firstly constructed the plasmid pTS1 from pJBEI-6409 [32] expressing the whole mevalonate pathway (Fig. S1), and transformed into *E. coli* BL21(DE3) to generate the base strain NCT with high production level of C_5 units DMAPP and IPP. Recombinant plasmid encoding *Sc*GPPC2MT wild type (WT) or variant G202X was individually transformed into strain NCT. Using the chemically synthesized 2-methyl-prenol (**1b**) standard as a positive control (Fig. 2C–i, 2D, and S3), we detected 2-methyl-prenol for five variants including G202M, G202F, G202W, G202H, and G202N (Fig. 2C–iii, iv, v, vi, vii, 2E, and S4), and not for *Sc*GPPC2MT WT or the control sample harboring an empty vector (Fig. 2C–viii, ix). The variant G202M exhibited the highest relative yield of 2-methyl-prenol (Fig. S5A). We reasoned that the non-polar linear side group of Met maintains a hydrophobic environment while acts as a clamp to shorten the hydrocarbon tail-binding tunnel to fit DMAPP. In support of this, M202 is ~3.6 Å away from hydrocarbon tail of DMAPP in a modeled structure with DMAPP docked at the substrate binding pocket, a distance comparable to that between G202 and the prenyl terminus of GPP (Fig. 2A, B). The results demonstrate synthesis of 2-methyl-DMAPP (**1a**) by those variants, and G202 as a key site to switch substrate specificity.

3.2. Improving the catalytic ability of ScGPPC2MT G202M to produce 2-methyl-DMAPP

The key residue F222 in the prenyl-binding groove of *Sc*GPPC2MT interacts with the 2,3-π bond of GPP via its aromatic ring and stabilizes the C3-tertiary carbocation intermediate through cation-π interactions [27]. Such an aromatic ring is conserved in GPP methyltransferases in the form of Phe or Tyr residue [14,27], while IPPMTs adopt a conserved Tyr residue (e.g., Y214 in *Sm*IPPMT) [20] (Fig. S2). Introduction of the F222Y into variant G202M led to a 3.3-fold increase in the relative yield of 2-methyl-prenol (Fig. 2C–ii, iii, and S5A). co-expression of the variant G202M-F222Y and a promiscuous phosphatase *Ec*NudB led to a titer of 1.03 mg/L for 2-methyl-prenol (Fig. S5B). Of note, no methylated C_5 molecule other than 2-methyl-prenol was detected, suggesting F222Y mutation did not change the substrate specificity. In the modeled structure of variant G202M-F222Y in complex with DMAPP, Y222 is positioned ~2.7 Å away from and predicted to form hydrogen bond with diphosphate group of DMAPP (Fig. 2B and S6). These evidences indicate that F222Y could contribute to stabilizing DMAPP via hydrogen bond interaction with the diphosphate group, and improves activity consequently.

The *in vitro* activity assay further confirmed that variant G202M-F222Y transformed DMAPP to its C2-methylated form (Fig. S7), and the steady-state kinetic parameters were $k_{cat}= (9.59 \pm 0.25) \times 10^{-5}\ s^{-1}$, $K_m = 5.33 \pm 0.81\ \mu M$, and $k_{cat}/K_m = 1.80 \times 10^{-5}\ \mu M^{-1}\ s^{-1}$ for DMAPP (Figs. S7–S9). Meanwhile, *Sc*GPPC2MT WT showed $k_{cat}= (4.90 \pm 0.16) \times 10^{-4}\ s^{-1}$, $K_m = 0.88 \pm 0.09\ \mu M$, and $k_{cat}/K_m = 5.59 \times 10^{-4}\ \mu M^{-1}\ s^{-1}$ for GPP (Fig. S7, S8, S10).

3.3. Incorperation of 2-methyl-DMAPP into higher trans- and cis-prenyl diphosphates

We next asked whether the new C_6 analog, 2-methyl-DMAPP, could be incorperated to genenrate longer chain (C_{5n+1}) prenyl diphosphates (Fig. 3A). Differing from 2-methyl-geraniol (**2b**) produced by *Sc*GPPC2MT WT (Fig. 3B–i and S11), a new peak was detected for variants G202M-F222Y and G202M, and matched with the 6-methyl-geraniol (**3b**) standard produced *in vivo* by GPPC6MT [14], the enzyme recently reported to methylate C6 of GPP (Fig. 3B–ii, ii, iv, and S12). Meanwhile, the ion $m/z = 83$ represents a characteristic fragment derived from 2-methyl-DMAPP (Fig. S12). Notably, the amount of 6-methyl-geraniol detected for variant G202M-F222Y was 7.9-fold higher than variant G202M (Fig. S13), while neither variant yielded 2-methyl-geraniol, in agreement with above results. Similarly, C_{16} alcohol 10-methyl-*E*, *E*-farnesol (**4b**) was detected for variants G202M-F222Y and G202M (Fig. 3C and S14). These data demonstrate *in vivo* synthesis of 6-methyl-GPP (**3a**) and 10-methyl-*E*, *E*-FPP (**4a**), and importantly, that IspA, the native FPP synthase catalyzing sequential formation of GPP and FPP in *E. coli*, recognizes 2-methyl-DMAPP as a substrate. For synthesis of 14-methyl-*E*, *E*, *E*-GGPP (**5a**), the geranylgeranyl diphosphate synthase from *Taxus canadensis* (*Tc*GGPPs) was additionally expressed but resulted in severe toxicity to cells. To leverage toxicity, *Tc*GGPPs was co-expressed with *Tb*TaxS, the taxa-4(5), 11(12)-diene synthase from *Taxus brevifolia* that converts GGPP to a key intermediate taxa-4(5),11(12)-diene in taxol biosynthesis [33], yielding a peak with mass spectrum consistent with C_{21} alcohol 14-methyl-*E*, *E*, *E*-geranylgeraniol (**5b**, Fig. 3D and S15).

Despite terpenoid biosynthesis in nature commonly uses prenyl diphosphates in *trans*-conformation, *cis*-prenyl diphosphates are produced in plants by *cis*–prenyltransferases (CPTs) and converted to terpenoids by *cis*-specific terpene synthases [34]. These were recently used to construct orthogonal terpenoid biosynthesis pathways with DMAPP and IPP as building blocks [35–37]. To explore whether 2-methyl-DMAPP can be used *cis*-terpene biosynthesis, we tested with CPT1 and CPT6 which synthesize neryl diphosphate (NPP, the *cis*-isomer of GPP) and *Z*, *Z*-FPP (the all-*cis*-isomer of *E*, *E*-FPP) respectively in *Solanum lycopersicum* [38,39]. Co-expression of *Sl*CPT1 and variant G202M-F222Y in *E. coli* NCT led to 6-methyl-nerol (**6b**), exhibiting the same ion fragment pattern as 6-methyl-genraiol (**3b**) but differing in retention time (Fig. 3E and S16). Similarly, a new peak consistent with 10-methyl-*Z*, *Z*-farnesol (**7b**) was detected upon co-expression of *Sl*CPT6 and variant G202M-F222Y (Fig. 3F and S17). Collectively, these data demonstrate acceptance of 2-methyl-DMAPP as a start unit to make noncanonical prenyl diphosphates in both *trans*- and *cis*-conformations.

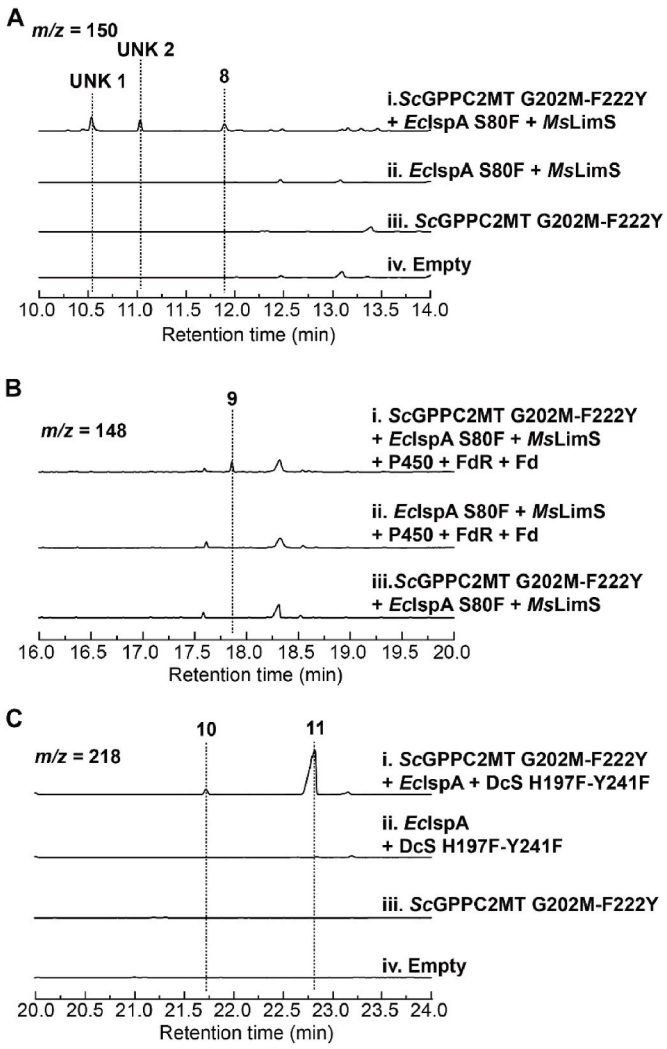

Fig. 4. Synthesis of noncanonical C_{11} and C_{16} terpenoids. (**A**) Production of C_{11} terpenes upon co-expression of *Sc*GPPC2MT G202M–F222Y, *Ec*IspA S80F, and *Ms*LimS. (**B**) Production of oxidized C_{11} terpenoid by further expression of an oxidation module containing cytochrome P450, FdR and Fd. (**C**) Analysis of C_{16} terpenes upon co-expression of *Sc*GPPC2MT G202M–F222Y, *Ec*IspA, and DcS H197F–Y241F. None of those compounds was detected in control strains expressing incomplete enzyme sets or containing empty vectors (empty).

3.4. Biosynthesis of terpenoids derived from 2-methyl-DMAPP

We further explored modification of prenyl diphosphates derived from 2-methyl-DMAPP by terpene synthases and cytochrome P450s to generate novel terpenoids. LimS is a well-studied terpene synthase converting GPP to limonene ($C_{10}H_{16}$) [40]. Upon binding and ionization of the GPP substrate, the diphosphate moiety migrates to C3, followed by rotation of the C2–C3 bond which brings C1 close to C6 for cyclization [40]. Despite rotation of the C2–C3 bond is the limiting step, LimS tolerates 2-methyl-GPP as a substrate and produces 2-methyl-limonene consequently [17]. Because of these features, we used LimS to test

acceptance of 6-methyl-GPP (**3a**) to generate 4-methyl-limonene. The IspA variant S80F was used to favor production of GPP instead of FPP [41]. Co-expression of *Ms*LimS, IspA S80F and variant G202M-F222Y resulted in three peaks (Fig. 4A, S18–S20). The mass spectrum of the peak eluted at 11.9 min is consistent with 4-methyl-limonene (**8**) (Fig. S20). The other two compounds (UNK1 and UNK2) were likely C_{11} terpenes with uncharacterized structures. When an oxidation module containing CYP153A6, the enzyme oxidizing limonene into perillyl alcohol ($C_{10}H_{16}O$), ferredoxin reductase (FdR), and ferredoxin (Fd) was further introduced, only one peak was detected with molecular and fragment ions consistent with methylated perillyl alcohol ($C_{11}H_{18}O$) (Fig. 4B and S21). Because oxidation of limonene by CYP153A6 occurs at C7 position [32], opposite to the C4 position where the methyl group is located in 4-methyl-limonene (**8**), CYP153A6 likely accepted 4-methyl-limonene as an alternative substrate and converted it to 4-methyl-perillyl alcohol (**9**). Additionally, expression of DcS H197F–Y241F, a variant of daucenol synthase (DcS) reported to cyclize chemically synthesized FPP analogs *in vitro* [42], led to two new peaks (Fig. 4C) with mass spectrum matching 4-epi-4-methyldauc-8-en-11-ol (**10**) and 3-methylwiddr-8-en-3-ol (**11**), respectively (Fig. S22, S23, ref. [42]).

4. Conclusion

By rational engineering the substrate binding pocket of a GPP C2-methyltransferase, we created an unprecedented DMAPP C2-methyltransferase that converts DMAPP to 2-methyl-DMAPP. The G202 in the prenyl diphosphate-binding groove acts as the key residue to switch substrate specificity, while F222Y substitution stabilizes substrate binding. This provides insights into substrate recognition and strategies to engineer prenyl diphosphate methyltransferase for alternated substrate spectrum. We further demonstrated *in vivo* incorporation of 2-methyl-DMAPP as a start unit to generate noncanonical prenyl diphosphates in both *trans*- and *cis*-configurations, and terpenoids. Application of 2-methyl-DMAPP opens new opportunities for extending structural and functional spaces of terpenoids. Additionally, 2-methyl-DMAPP may be applied to study prenylation that is a common modification occurring to tRNA, proteins, and natural products other than terpenoids.

Credit author statement

Chen-Yang Xia: Conceptualization, Methodology, Investigation, Writing – original draft, Visualization. **Bo-Wen Lu**: Methodology, Investigation. **Ji-Yun Cui**: Visualization. **Bai-Yang Wang**: Investigation. **Yue-Yang Sun**: Investigation. **Fei Gan**: Conceptualization, Writing – original draft, Writing – review & editing, Visualization, Supervision, Project administration, Funding acquisition.

Declaration of competing interest

We have no conflict of interest to declare.

Acknowledgement

We thank Dr. Yuhui Sun at School of Pharmaceutical Sciences, Wuhan University for kindly providing strain *Streptomyces coelicolor*. We also thank Dr. Bo Pang for helpful discussion and suggestion on this manuscript. This work was supported in part by the National Key R&D Program of China (2021YFA0909600 and 2019YFA0909400).

Appendix A. Supplementary data

Supplementary data to this article can be found online at https://doi.org/10.1016/j.synbio.2022.12.002.

References

[1] Ro DK, Paradise EM, Ouellet M, Fisher KJ, Newman KL, Ndungu JM, et al. Production of the antimalarial drug precursor artemisinic acid in engineered yeast. Nature 2006;440:940–3. https://doi.org/10.1038/nature04640.
[2] Luo X, Reiter MA, d'Espaux L, Wong J, Denby CM, Lechner A, et al. Complete biosynthesis of cannabinoids and their unnatural analogues in yeast. Nature 2019;567:123–6. https://doi.org/10.1038/s41586-019-0978-9.
[3] Westfall PJ, Pitera DJ, Lenihan JR, Eng D, Woolard FX, Regentin R, et al. Production of amorphadiene in yeast, and its conversion to dihydroartemisinic acid, precursor to the antimalarial agent artemisinin. Proc Natl Acad Sci U S A 2012;109:E111–8. https://doi.org/10.1073/pnas.1110740109.
[4] Vickers CE, Williams TC, Peng B, Cherry J. Recent advances in synthetic biology for engineering isoprenoid production in yeast. Curr Opin Chem Biol 2017;40:47–56. https://doi.org/10.1016/j.cbpa.2017.05.017.
[5] Pichersky E, Noel JP, Dudareva N. Biosynthesis of plant volatiles: nature's diversity and ingenuity. Science 2006;311:808–11. https://doi.org/10.1126/science.1118510.
[6] Chen R, Jia Q, Mu X, Hu B, Sun X, Deng Z, et al. Systematic mining of fungal chimeric terpene synthases using an efficient precursor-providing yeast chassis. Proc Natl Acad Sci U S A 2021;118. https://doi.org/10.1073/pnas.2023247118.
[7] Tao H, Lauterbach L, Bian G, Chen R, Hou A, Mori T, et al. Discovery of non-squalene triterpenes. Nature 2022;606:414–9. https://doi.org/10.1038/s41586-022-04773-3.
[8] Bian G, Han Y, Hou A, Yuan Y, Liu X, Deng Z, et al. Releasing the potential power of terpene synthases by a robust precursor supply platform. Metab Eng 2017;42:1–8. https://doi.org/10.1016/j.ymben.2017.04.006.
[9] Eiben CB, de Rond T, Bloszies C, Gin J, Chiniquy J, Baidoo EEK, et al. Mevalonate pathway promiscuity enables noncanonical terpene production. ACS Synth Biol 2019;8:2238–47. https://doi.org/10.1021/acssynbio.9b00230.
[10] Von Reuss S, Domik D, Lemfack MC, Magnus N, Kai M, Weise T, et al. Sodorifen biosynthesis in the rhizobacterium *Serratia plymuthica* involves methylation and cyclization of MEP-derived farnesyl pyrophosphate by a SAM-dependent C-methyltransferase. J Am Chem Soc 2018;140:11855–62. https://doi.org/10.1021/jacs.8b08510.
[11] Komatsu M, Tsuda M, Omura S, Oikawa H, Ikeda H. Identification and functional analysis of genes controlling biosynthesis of 2-methylisoborneol. Proc Natl Acad Sci U S A 2008;105:7422–7. https://doi.org/10.1073/pnas.0802312105.
[12] Wang CM, Cane DE. Biochemistry and molecular genetics of the biosynthesis of the earthy odorant methylisoborneol in *Streptomyces coelicolor*. J Am Chem Soc 2008;130:8908–9. https://doi.org/10.1021/ja803639g.
[13] Dickschat JS, Nawrath T, Thiel V, Kunze B, Muller R, Schulz S. Biosynthesis of the off-flavor 2-methylisoborneol by the myxobacterium *Nannocystis exedens*. Angew Chem Int Ed Engl 2007;46:8287–90. https://doi.org/10.1002/anie.200702496.
[14] Tsutsumi H, Moriwaki Y, Terada T, Shimizu K, Shin-Ya K, Katsuyama Y, et al. Structural and molecular basis of the catalytic mechanism of geranyl pyrophosphate C6-methyltransferase: creation of an unprecedented farnesyl pyrophosphate C6-methyltransferase. Angew Chem Int Ed Engl 2022;61:e202111217. https://doi.org/10.1002/anie.202111217.
[15] Ozaki T, Shinde SS, Gao L, Okuizumi R, Liu C, Ogasawara Y, et al. Enzymatic formation of a skipped methyl-substituted octaprenyl side chain of longestin (KS-505a): involvement of homo-IPP as a common extender unit. Angew Chem Int Ed Engl 2018;57:6629–32. https://doi.org/10.1002/anie.201802116.
[16] Pang B, Li J, Eiben CB, Oksen E, Barcelos C, Chen R, et al. Lepidopteran mevalonate pathway optimization in *Escherichia coli* efficiently produces isoprenol analogs for next-generation biofuels. Metab Eng 2021;68:210–9. https://doi.org/10.1016/j.ymben.2021.10.007.
[17] Ignea C, Pontini M, Motawia MS, Maffei ME, Makris AM, Kampranis SC. Synthesis of 11-carbon terpenoids in yeast using protein and metabolic engineering. Nat Chem Biol 2018;14:1090–8. https://doi.org/10.1038/s41589-018-0166-5.
[18] Takagi C, Abe M, Kaneko Y, Sasaki A, Ito A, Sakemi Y, et al. Structures of new C41 carotenoids produced using recombinant *Escherichia coli* expressing genes encoding isopentenyl pyrophosphate, methyltransferase, and carotenoid biosynthetic enzymes. Tetrahedron Lett 2020;61:152633. https://doi.org/10.1016/j.tetlet.2020.152633.
[19] Kschowak MJ, Wortmann H, Dickschat JS, Schrader J, Buchhaupt M. Heterologous expression of 2-methylisoborneol/2 methylenebornane biosynthesis genes in *Escherichia coli* yields novel C11-terpenes. PLoS One 2018;13:e0196082. https://doi.org/10.1371/journal.pone.0196082.
[20] Drummond L, Kschowak MJ, Breitenbach J, Wolff H, Shi YM, Schrader J, et al. Expanding the isoprenoid building block repertoire with an IPP methyltransferase from *Streptomyces monomycini*. ACS Synth Biol 2019;8:1303–13. https://doi.org/10.1021/acssynbio.8b00525.
[21] Drummond L, Haque PJ, Gu B, Jung JS, Schewe H, Dickschat JS, et al. High versatility of IPP and DMAPP methyltransferases enables synthesis of C6 , C7 and C8 terpenoid building blocks. Chembiochem 2022;23:e202200091. https://doi.org/10.1002/cbic.202200091.
[22] Tamura K, Stecher G, Kumar S. MEGA11: molecular evolutionary genetics analysis version 11. Mol Biol Evol 2021;38:3022–7. https://doi.org/10.1093/molbev/msab120.
[23] Waterhouse A, Bertoni M, Bienert S, Studer G, Tauriello G, Gumienny R, et al. SWISS-MODEL: homology modelling of protein structures and complexes. Nucleic Acids Res 2018;46:W296–303. https://doi.org/10.1093/nar/gky427.
[24] Morris GM, Huey R, Lindstrom W, Sanner MF, Belew RK, Goodsell DS, et al. Autodock4 and Autodocktools4: automated docking with selective receptor flexibility. J Comput Chem 2009;30:2785–91. https://doi.org/10.1002/jcc.21256.

[25] Delano WL. The PyMOL molecular graphics system. 2002.
[26] Schoning-Stierand K, Diedrich K, Fahrrolfes R, Flachsenberg F, Meyder A, Nittinger E, et al. ProteinsPlus: interactive analysis of protein-ligand binding interfaces. Nucleic Acids Res 2020;48:W48–53. https://doi.org/10.1093/nar/gkaa235.
[27] Koksal M, Chou WK, Cane DE, Christianson DW. Structure of geranyl diphosphate C-methyltransferase from *Streptomyces coelicolor* and implications for the mechanism of isoprenoid modification. Biochemistry 2012;51:3003–10. https://doi.org/10.1021/bi300109c.
[28] Ariyawutthiphan O, Ose T, Minami A, Shinde S, Tsuda M, Gao YG, et al. Structure analysis of geranyl pyrophosphate methyltransferase and the proposed reaction mechanism of SAM-dependent C-methylation. Acta Crystallogr D Biol Crystallogr 2012;68:1558–69. https://doi.org/10.1107/S0907444912038486.
[29] Chou HH, Keasling JD. Synthetic pathway for production of five-carbon alcohols from isopentenyl diphosphate. Appl Environ Microbiol 2012;78:7849–55. https://doi.org/10.1128/AEM.01175-12.
[30] Withers ST, Gottlieb SS, Lieu B, Newman JD, Keasling JD. Identification of isopentenol biosynthetic genes from *Bacillus subtilis* by a screening method based on isoprenoid precursor toxicity. Appl Environ Microbiol 2007;73:6277–83. https://doi.org/10.1128/AEM.00861-07.
[31] Zada B, Wang C, Park JB, Jeong SH, Park JE, Singh HB, et al. Metabolic engineering of *Escherichia coli* for production of mixed isoprenoid alcohols and their derivatives. Biotechnol Biofuels 2018;11:210. https://doi.org/10.1186/s13068-018-1210-0.
[32] Alonso-Gutierrez J, Chan R, Batth TS, Adams PD, Keasling JD, Petzold CJ, et al. Metabolic engineering of *Escherichia coli* for limonene and perillyl alcohol production. Metab Eng 2013;19:33–41. https://doi.org/10.1016/j.ymben.2013.05.004.
[33] Ajikumar PK, Xiao WH, Tyo KE, Wang Y, Simeon F, Leonard E, et al. Isoprenoid pathway optimization for taxol precursor overproduction in *Escherichia coli*. Science 2010;330:70–4. https://doi.org/10.1126/science.1191652.
[34] Zhou F, Pichersky E. More is better: the diversity of terpene metabolism in plants. Curr Opin Plant Biol 2020;55:1–10. https://doi.org/10.1016/j.pbi.2020.01.005.
[35] Ignea C, Raadam MH, Motawia MS, Makris AM, Vickers CE, Kampranis SC. Orthogonal monoterpenoid biosynthesis in yeast constructed on an isomeric substrate. Nat Commun 2019;10:3799. https://doi.org/10.1038/s41467-019-11290-x.
[36] Zi J, Matsuba Y, Hong YJ, Jackson AJ, Tantillo DJ, Pichersky E, et al. Biosynthesis of lycosantalonol, a *cis*-prenyl derived diterpenoid. J Am Chem Soc 2014;136:16951–3. https://doi.org/10.1021/ja508477e.
[37] Matsuba Y, Zi J, Jones AD, Peters RJ, Pichersky E. Biosynthesis of the diterpenoid lycosantalonol via nerylneryl diphosphate in *Solanum lycopersicum*. PLoS One 2015;10:e0119302. https://doi.org/10.1371/journal.pone.0119302.
[38] Schilmiller AL, Schauvinhold I, Larson M, Xu R, Charbonneau AL, Schmidt A, et al. Monoterpenes in the glandular trichomes of tomato are synthesized from a neryl diphosphate precursor rather than geranyl diphosphate. Proc Natl Acad Sci U S A 2009;106:10865–70. https://doi.org/10.1073/pnas.0904113106.
[39] Akhtar TA, Matsuba Y, Schauvinhold I, Yu G, Lees HA, Klein SE, et al. The tomato *cis*-prenyltransferase gene family. Plant J 2013;73:640–52. https://doi.org/10.1111/tpj.12063.
[40] Hyatt DC, Youn B, Zhao Y, Santhamma B, Coates RM, Croteau RB, et al. Structure of limonene synthase, a simple model for terpenoid cyclase catalysis. Proc Natl Acad Sci U S A 2007;104:5360–5. https://doi.org/10.1073/pnas.0700915104.
[41] Reiling KK, Yoshikuni Y, Martin VJ, Newman J, Bohlmann J, Keasling JD. Mono and diterpene production in *Escherichia coli*. Biotechnol Bioeng 2004;87:200–12. https://doi.org/10.1002/bit.20128.
[42] Lauterbach L, Hou A, Dickschat JS. Rerouting and improving dauc-8-en-11-ol synthase from *Streptomyces venezuelae* to a high yielding biocatalyst. Chemistry 2021;27:7923–9. https://doi.org/10.1002/chem.202100962.